Title
Tropospheric Reactive Odd Nitrogen Over the South Pacific in Austral Springtime

Journal
Journal of Geophysical Research, 105(3)

Authors
Blake, DR
Talbot, RW
Dibb, JE
et al.

Publication Date
2000

JOURNAL OF GEOPHYSICAL RESEARCH, VOL. 105, NO. D5, PAGES 6681-6694, MARCH 16, 2000

Tropospheric reactive odd nitrogen over the South Pacific in austral springtime

R. W. Talbot,[1] J. E. Dibb,[1] E. M. Scheuer,[1] J. D. Bradshaw,[2,3] S. T. Sandholm,[2]
H. B. Singh,[4] D. R. Blake,[5] N. J. Blake,[5] E. Atlas,[6] and F. Flocke[6]

Abstract. The distribution of reactive nitrogen species over the South Pacific during austral springtime appears to be dominated by biomass burning emissions and possibly lightning and stratospheric inputs. The absence of robust correlations of reactive nitrogen species with source-specific tracers (e.g., C_2H_2 [combustion], CH_3Cl [biomass burning], C_2Cl_4 [industrial], ^{210}Pb [continental], and ^7Be [stratospheric]) suggests significant aging and processing of the sampled air parcels due to losses by surface deposition, OH attack, and dilution processes. Classification of the air parcels based on CO enhancements indicates that the greatest influence was found in plumes at 3-8 km altitude in the distributions of HNO_3 and peroxyacetyl nitrate (PAN). Here mixing ratios of these species reached 600 parts per trillion by volume (pptv), values surprisingly large for a location several thousand kilometers removed from the nearest continental areas. The mixing ratio of total reactive nitrogen (the NO_y sum), operationally defined in this paper as measured (NO + HNO_3 + PAN + CH_3ONO_2 +$C_2H_5ONO_2$) + modeled (NO_2), had a median value of 285 pptv within these plumes compared with 120 pptv in nonplume air parcels. Particle NO_3^- was not included in this analysis of the NO_y sum due to its 10- to 15-min sampling time resolution, but, in general, it was <10% of the NO_y sum. Comparison of the two air parcel classifications for NO_x and alkyl nitrate distributions showed no perceivable plume influence, but recycling of reactive nitrogen may have masked this direct effect. In the marine boundary layer, the NO_y sum averaged 50 pptv in both air parcel classifications, being somewhat isolated from the polluted conditions above it by the trade wind inversion. In this region, however, alkyl nitrates appear to have an important marine source where they comprise 20-80% of the NO_y sum in equatorial and high-latitude regions over the South Pacific.

1. Introduction

Reactive odd nitrogen species play central roles in tropospheric photochemistry. The concentration of NO_x (NO + NO_2) controls photochemical production or destruction of O_3, and it also influences the concentration of HO_x (OH + HO_2). Ozone and HO_x are important since they largely determine the oxidizing capacity of the troposphere. Because of the high chemical reactivity of NO_x, it is often converted photochemically to HNO_3 and the reservoir species peroxyacetyl nitrate (PAN). These conversions take place in a matter of hours during the summertime [*Logan*, 1983; *Kasting and Singh*, 1986]. Reactive nitrogen can be transported over long distances as HNO_3 and PAN, and they may eventually react to regenerate NO_x in remote areas. Removal of reactive nitrogen from the troposphere is primarily by wet and dry deposition of HNO_3 and particle NO_3^- [*Logan*, 1983].

Total reactive odd nitrogen (NO_y) has been defined as the sum of the individual species which are reactive in the troposphere. These species include NO, NO_2, NO_3, N_2O_5, HNO_3, HONO, PAN, $RONO_2$ (R= alkyl), and particle NO_3^-. Together this suite of compounds has also been estimated by measurement of NO_y as NO using a gold catalytic converter and a reductant such as CO [*Bradshaw et al.*, 1998]. In air parcels without recent emission inputs these two measures of NO_y often disagree [*Fahey et al.*, 1986; *Atlas et al.*, 1992a; *Sandholm et al.*, 1994 ; *Bradshaw et al.*, 1998]. Some of these differences may be due to certain species, such as organic nitrates, not being measured on an individual basis, but they are still included in the more general NO_y measurement [e.g., *Atlas et al.*, 1992a]. In addition, some NO_y converters appear to convert non-NO_y compounds (e.g., NH_3 and HCN) with varying efficiency [*Kliner et al.*, 1997; *Bradshaw et al.*, 1998]. However, surprisingly good agreement in measured NO_y and the NO_y sum was found recently for the upper troposphere over the North Atlantic [*Talbot et al.*, 1999a]. The reasons for varying degrees of agreement are unclear, and it may be more meaningful to measure the individual species and use their sum as representative of NO_y (the NO_y sum). This approach has been adopted by the NASA Global Tropospheric Experiment (GTE) program and is the one used in this paper.

The distribution of reactive odd nitrogen species and the mechanisms that control their concentrations are not well understood for large areas of the global troposphere. This is particularly

[1]Institute for the Study of Earth, Oceans and Space, University of New Hampshire, Durham.
[2]Department of Earth and Atmospheric Sciences, Georgia Institute of Technology, Atlanta.
[3]Deceased June 16, 1997.
[4]NASA Ames Research Center, Moffett Field, California.
[5]Department of Chemistry, University of California-Irvine.
[6]Atmospheric Chemistry Division, National Center for Atmospheric Research, Boulder, Colorado.

Paper number 1999JD901114.
0148-0227/00/1999JD901114$09.00

true for the South Pacific, and as such these measurements were an integral component of the NASA Pacific Exploratory Mission-Tropics (PEM-Tropics) A airborne expedition over this region during September-October 1996. This paper presents the distributions and interrelations of measured NO, HNO_3, PAN, CH_3ONO_2, and $C_2H_5ONO_2$ plus modeled NO_2 over the South Pacific during PEM-Tropics A.

2. Experimental Methods

2.1. Study Area

The PEM-Tropics A airborne expedition was conducted using the NASA Ames DC-8 research aircraft. Transit and intensive site science missions comprised 18 flights, averaging 8-10 hours in duration and covering the altitude range of 0.3-12.5 km. The base of operations progressed as follows: (1) Tahiti (three missions), (2) Easter Island (two missions), (3) Tahiti (one mission), (4) New Zealand (one mission), and (5) Fiji (three missions). The overall scientific rationale and description of individual aircraft missions are described in the PEM-Tropics A overview paper [*Hoell et al.*, 1999]. The features of the large-scale meteorological regime and associated air mass trajectory analyses for the September-October 1996 period are presented by *Fuelberg et al.* [1999]. The data used in this paper were obtained in the geographic grid approximately bounded by 60°N - 75°S latitude and 165°E - 105°W longitude. A geographic map with the flight location details is shown in several prior papers [e.g., *Hoell et al.*, 1999]. The measured and model-calculated parameters utilized in the present paper are available from the NASA Langley Distributed Data Archive Center (DDAC) or the GTE project archive (ftp-gte.larc.nasa.gov).

2.2. Sampling and Analytical Methodology

2.2.1. NO. Nitric oxide was measured with the Georgia Tech two-photon/laser-induced fluorescence instrument [*Bradshaw et al.*, 1985; *Sandholm et al.*, 1990]. This technique is spectroscopically selective for NO. The system incorporated recent advancements in laser detection hardware as well as improvements in the airborne sampling manifold [*Bradshaw et al.*, 1999]. The inlet consisted of a 100-mm ID glass-coated stainless steel flow system which skimmed and dumped to exhaust the air flow nearest the walls. The inlet was mounted in a 45°orientation to the fuselage and utilized a ram air flow rate of 40,000 L min^{-1}. This high flow rate created a "pseudo-wall-less" sampling environment in that nearly all NO_y species that may have interacted with the walls would not have time to make it back to the volume element being sampled in the central core of the manifold before being exhausted overboard. Thus NO was measured in the center core flow only, minimizing potential wall artifacts [*Bradshaw et al.*, 1999]. Wall effects were also greatly reduced by steering the two probe beams (sampling an area of <1 cm^2) through the center of the sampling manifold which itself had a cross-sectional area of ~80 cm^2. Given a 10-Hz probe frequency, this high flow rate also permitted adequate time for a complete turnover of the sampling region between laser shots, thus ensuring that measurements of NO were being made under true ambient conditions. The measurements were reported using an integration time of 1 s. Accuracy of the instrument calibration is estimated to be ±16% for NO at the 95% confidence limit.

2.2.2. NO_2. Model-calculated NO_2 was used here instead of the Georgia Tech measured NO_2 due to better time overlap with the other NO_y sum measurements. It should be noted that the measured and modeled NO_2 data were highly correlated, giving a $(NO_2)_{meas}/(NO_2)_{calc}$ ratio of 0.93 [*Bradshaw et al.*, 1999]. The Harvard photochemical point model was used to calculate NO_2 along the DC-8 flight path from diurnal steady state concentrations of radicals and chemical intermediates estimated using the ensemble of observations from the aircraft [*Schultz et al.*, 1999].

2.2.3. HNO_3. Acidic gases were subsampled from a high-volume (500-1500 standard liters per minute sLpm) flow of ambient air using the mist chamber technique [*Talbot et al.*, 1997a; *Talbot et al.*, 1999b]. The subsample flow rate was always <10% of the primary manifold total flow. Sample collection intervals were typically 4 min in the boundary layer, 6 min at 2-9 km altitude, and 8 min above 9 km altitude, reflecting decreased pumping rates in the middle and upper troposphere. The inlet manifold consisted of a 0.9-m length of 41-mm ID glass-coated stainless steel pipe. The pipe extended from the DC-8 fuselage to provide a 90° orientation to the ambient air streamline flow. To facilitate pumping of the high-volume manifold flow on both the HNO_3 and Georgia Tech systems, a diffuser was mounted over the end of the inlet pipe parallel to the DC-8 fuselage. This device provided a "shroud" effect, slowing the flow of ambient air through it to slightly below the true air speed of the DC-8 and adding 50-100 hPa of pressurization to the sampling manifold. This effectively eliminated the reverse venturi effect (~40 hPa) on the sampling manifold. An additional feature of the diffuser was a curved step around the manifold pipe, which provided the streamline effects of a backward facing inlet. Its function was to facilitate exclusion of aerosol particles greater than ~2 μm in diameter from the sampling manifold. Aerosols smaller than this were removed from the sampled airstream using a 1-μm pore-sized Zefluor Teflon filter that was readily changeable every 5-10 min to minimize aerosol loading on the filter and gas/aerosol phase partitioning from ambient conditions. The accuracy of the HNO_3 measurements is estimated to be ±20%, with a precision ranging from ±10 to 35% depending on the ambient mixing ratio.

2.2.4. PAN. The NASA Ames PAN instrument provided measurements of this species using electron capture gas chromatography detection from a cryogenically enriched sample of ambient air [*Singh and Salas*, 1983; *Gregory et al.*, 1990]. The system uses an aft facing Teflon inlet with the instrument operated at a constant pressure of 1050 mbar isolated from aircraft cabin pressure fluctuations. The sampling time of 2 min was followed by a 5-min analysis time. In-flight calibration was accomplished using PAN synthesized in liquid *n*-tridecane. The PAN measurements have an estimated accuracy of about ±20% and a precision of ±10%. The detection limit for PAN was 2-3 parts per trillion by volume (pptv).

2.2.5 Alkyl Nitrates. C_1-C_4 alkyl nitrates were collected in stainless steel canisters and then separated analytically on a Restek-1701 column and quantified by electron capture detection [*Atlas et al.*, 1992b]. Oxygen doping enhanced the sensitivity of the electron capture detection for the alkyl nitrates. The precision is ±5% at mixing ratios above 5 pptv and ±10% below this value.

3. Results

3.1. Database

The data in this paper used the timescale defined by the HNO_3 measurements, with all other species (including calculated NO_2) averaged to this time base. The data set was further refined by using only time periods where there was a measurement reported for all the reactive nitrogen species. This reduced the size of the merged product by about 50%, but it still allowed meaningful comparisons for the NO_y sum with other parameters, as data from each mission and a wide altitude span were included. Again, for the purposes of

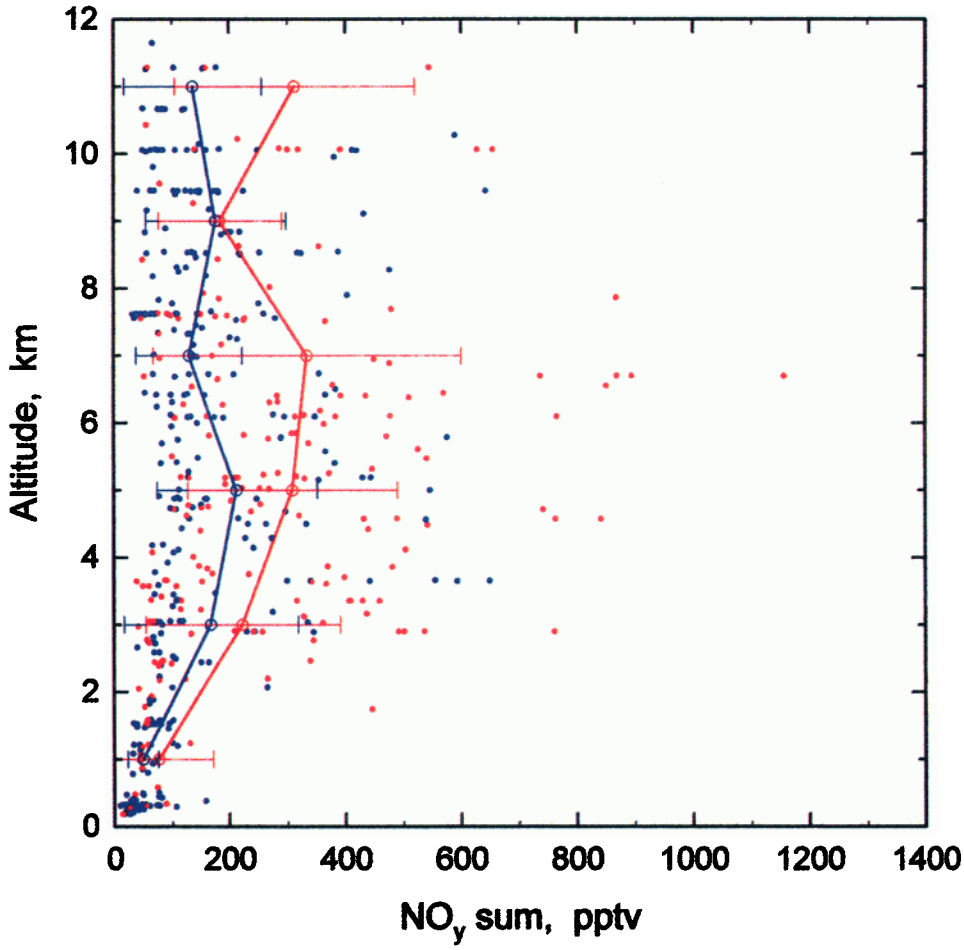

Plate 1. Vertical distribution of the NO_y sum in nonplume and plume air parcel classifications. Blue dots are nonplume data, and red dots are from within combustion plumes. The open circles represent the average value ± one standard deviation for 2 km altitude bins.

this paper, NO_y is defined as the sum (the NO_y sum) of the individual species NO, HNO_3, PAN, CH_3ONO_2, $C_2H_5ONO_2$ plus model-calculated NO_2. The higher alkyl nitrate species were <1 pptv and present inconsistently, so they are not included in this analysis of the NO_y sum.

Because of the significant impact of aged biomass burning emissions over the South Pacific in austral springtime [*Gregory et al.*, 1999; *Schultz et al.*, 1999; *Talbot et al.*, 1999b], the data were divided into two groups: (1) within biomass combustion plumes and (2) nonplume air parcels. The combustion data set corresponds to sampling times where CO was enhanced >10 ppbv in plumes well defined by CO, O_3, C_2H_2, and C_2H_6 (*J. A. Logan et al.*, manuscript in preparation, 1999).

Although not discussed in detail this paper, particle NO_3^- mixing ratios were generally <50 pptv [*Dibb et al.*, 1999a]. The time resolution of these measurements was typically 10-15 min, so their inclusion in the NO_y discussion in this paper is difficult. In only a few cases in the combustion plume data set was particle NO_3^- greater than 10% of the NO_y sum. It appears that wet scavenging of particle NO_3^- occurred early in the life of the biomass burning emissions, with only an occasional plume containing >50 pptv of particle NO_3^- [*Dibb et al.*, 1999b].

3.2. Vertical Distributions

Figure 1 illustrates the vertical distribution encountered commonly over the South Pacific for species associated with combustion emissions. This plume was encountered west of Tahiti on a spiral ascent during mission 6 and was particularly well defined by C_2H_2, a unique tracer of combustion emissions [*Blake et al.*, 1996a]. Note that C_2Cl_4, an industrial emissions tracer, was not elevated between 3 and 6 km altitude with the other trace gases. The biomass burning tracer CH_3Cl [*Blake et al.*, 1996b] fluctuated between 550 and 575 pptv over the entire spiral altitude but did not show a pronounced plume like the other combustion-associated species. In other cases, CH_3Cl exhibited a higher correlation with these species in plumes. The large-scale distribution of nonmethane hydrocarbons and selected halocarbons over the South Pacific during PEM-Tropics A is presented elsewhere [*Blake et al.*, 1999], where multiple spiral data illustrate the apparent impact of biomass burning emissions in the middle and upper troposphere.

It is important to recognize that the plumes sampled during PEM-Tropics A were aged from 1 to 2.5 weeks since they last passed over land based on model calculations of air parcel trajectories [*Fuelberg et al.*, 1999] and independent estimates using a combination of radioactive ingrowth of ^{210}Pb and OH decomposition of selected hydrocarbons [*Dibb et al.*, 1999b]. The air parcels sampled over the South Pacific last passed over land in Africa, Australia, or Indonesia, all regions of active biomass burning during austral springtime [*Fuelberg et al.*, 1999]. In addition, lightning associated with convection in these areas was very abundant [*Fuelberg et al.*, 1999], and it could have contributed reactive nitrogen to the plumes that we encountered over the South Pacific.

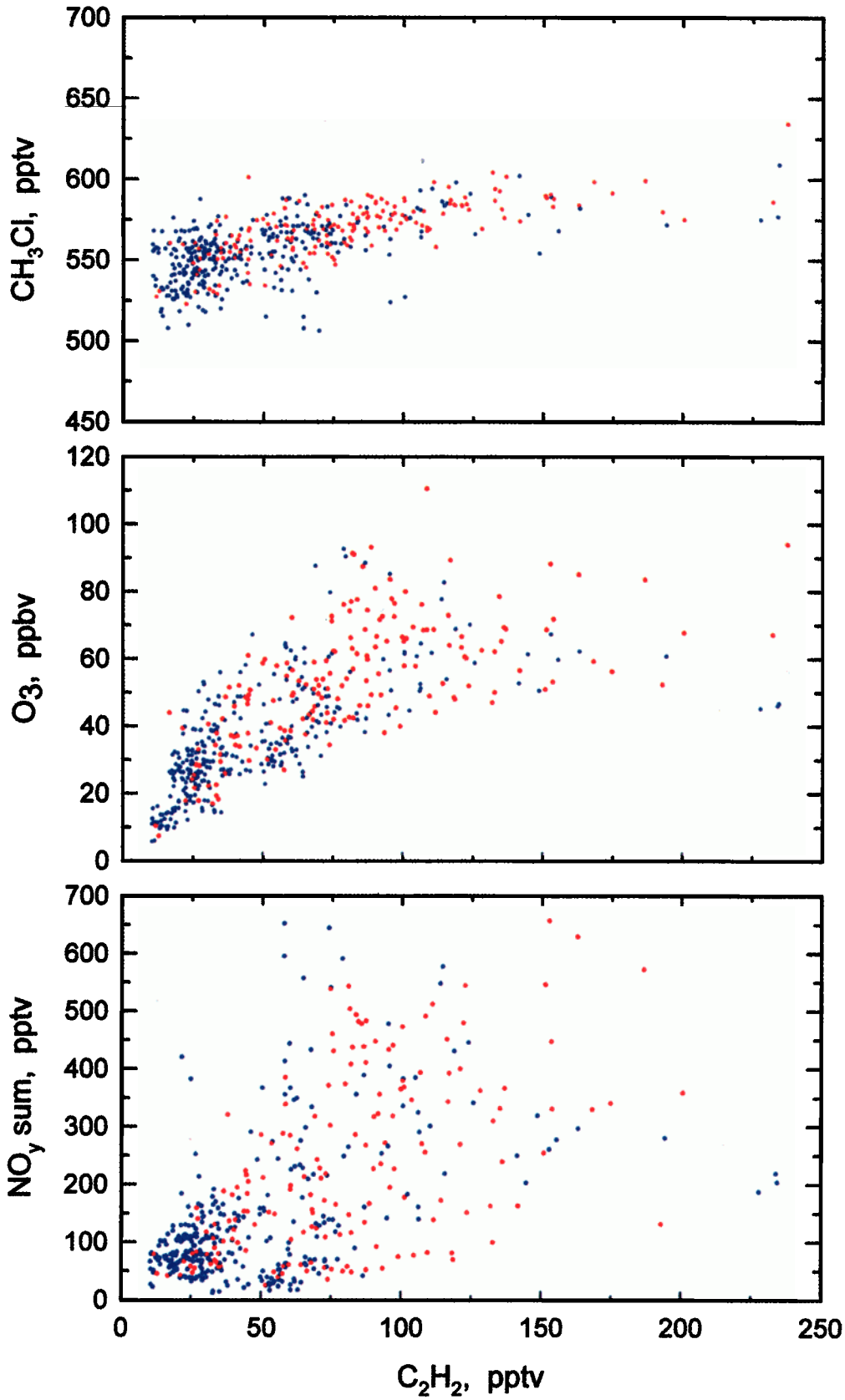

Plate 2. Relationship between selected species and C_2H_2 over the South Pacific. Blue dots are nonplume data, and red dots are from within combustion plumes.

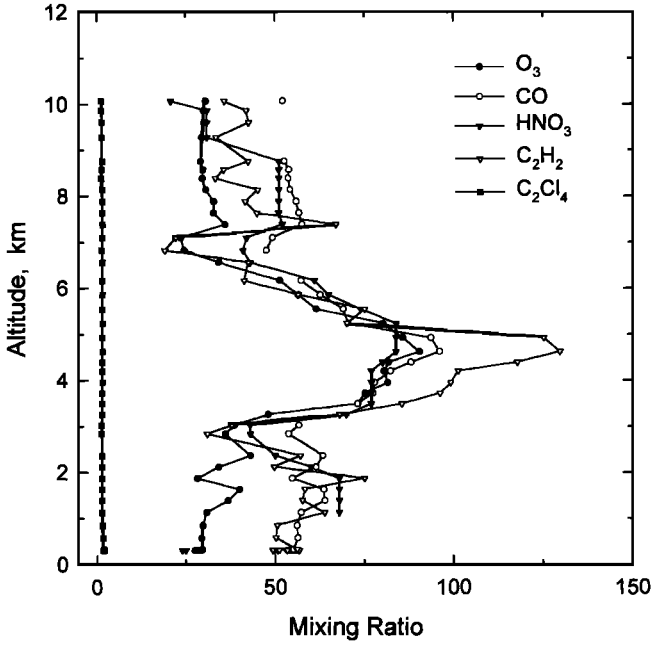

Figure 1. Vertical distribution of selected trace gases during a spiral ascent on mission 6 just west of Tahiti at 15°S and 155°W. Mixing ratios of O_3 and CO are in parts per billion by volume, and the other species are in parts per trillion by volume.

It was rare to find elevated NO_x mixing ratios in these plumes due to the potentially long time periods from its injection from combustion or lightning over continental areas. During transport of this duration it should have been converted to HNO_3, PAN, and possibly other reactive nitrogen forms. Indeed, the absence of significant aerosols in these plumes but elevated mixing ratios of HNO_3 (e.g., Figure 1) indicate photochemical production of HNO_3 during long-range transport after being scavenged initially by convection over continental areas [*Talbot et al.*, 1999b].

The vertical distributions of NO_x, HNO_3, PAN, CH_3ONO_2, and $C_2H_5ONO_2$ over the South Pacific are presented in Figures 2a (nonplume) and 2b (within plumes). In general, the mixing ratio of NO_x in nonplume air parcels was <50 pptv, with much of the data <20 pptv. Mixing ratios were <5 pptv in the marine boundary layer, increasing to an average of 25 pptv in the upper troposphere. It was not uncommon to have areas in the marine boundary layer where the mixing ratio of NO was <1 pptv and as low as 0.2 pptv [*Bradshaw et al.*, 1999].

The mixing ratios of HNO_3 and PAN were usually <100 pptv, but larger departures from this value are evident in the nonplume air parcels. Notice that in the middle troposphere (3-10 km), HNO_3 and PAN are both present at several hundred parts per trillion by volume. In the marine boundary layer, PAN was <5 pptv and HNO_3 was <20 pptv. Thermal decomposition of PAN occurs on the order of hours in this warm (25°-30°C), moist region, which should lead to HNO_3 production from the NO_2 + OH mechanism. The mixing ratio of HNO_3 is, however, kept <20 pptv due to its deposition to the ocean and uptake onto salt aerosol in the boundary layer [*Talbot et al.*, 1999b]. Below 4 km altitude the NO_x responsible for O_3 production is largely explained by the decomposition of PAN [*Schultz et al.*, 1999].

The mixing ratios of NO_x, HNO_3, and PAN in the nonplume air parcels over the South Pacific in the middle and upper troposphere were comparable to those typically found at remote locations. NO_x, HNO_3, and PAN are typically 50-100 pptv at Mauna Loa [*Atlas et al.*, 1992a] and over the North Pacific in aged marine air [*Talbot et al*, 1996a, 1997b]. The principal difference in the reactive nitrogen distributions over these Pacific regions is for NO_x in the marine boundary layer. With the South Pacific being by far the most remote of these locations, NO_x mixing ratios are twofold to fivefold lower.

The alkyl nitrate distribution over the South Pacific was dominated by CH_3ONO_2, which averaged from 15 pptv in the marine boundary layer to around 10 pptv from 2 to 12 km altitude. The only other significant alkyl nitrate was $C_2H_5ONO_2$, with its distribution mainly <5 pptv at all altitudes.

Looking at the vertical distributions of reactive nitrogen species in the combustion plume air parcels (Figure 2b) shows that NO_x was very similar to the nonplume group. The difference in the two groups' altitude bin means is <10 pptv above 2 km, with the plume data exhibiting the slightly higher values. The differences are even less for the two alkyl nitrates but in the opposite direction, with about 3 pptv less, on average, in the plume data vertical distribution of CH_3ONO_2.

The largest differences in the vertical distributions between the two groups is in the middle troposphere where HNO_3 and PAN were enhanced in the plume data set. The greatest mixing ratios of HNO_3 and PAN were observed in the 2-8 km altitude region. We found average mixing ratios of HNO_3 of 175 pptv and 165 pptv for PAN compared with 100 and 50 pptv, respectively, in the nonplume air parcels. Mixing ratios of HNO_3 and PAN around 500 pptv over the South Pacific are among the largest ever observed in the remote middle troposphere (Figure 2b). This is quite remarkable considering that the South Pacific is one of the most isolated locations on Earth. Here the large-scale flow pattern dominated by westerlies [*Fuelberg et al.*, 1999] apparently brings quite aged continentally derived combustion emissions to the South Pacific during the austral springtime period. This source influence is barely perceivable in NO_x and alkyl nitrates but is easily noticeable in HNO_3 and PAN.

The vertical distributions of the NO_y sum in the nonplume and plume air parcel classifications are shown in Plate 1. In the marine boundary, which is somewhat isolated from the polluted conditions above it by the trade wind inversion, the NO_y sum averaged ~50 pptv in both air parcel types. The impact of the combustion plumes was significant from 2 to 12 km altitude. In this region, the NO_y sum averaged 285 pptv in the plumes compared with 120 pptv in nonplume air parcels. Values of the NO_y sum of 100-150 pptv are typical of air parcels over remote regions not recently influenced by emission sources [*Atlas et al*, 1992a; *Ridley*, 1991; *Talbot et al*, 1996a, 1997b, 1999a].

3.3. NO_y Partitioning

To examine the relationship of various species to NO_y, the vertical distributions of their ratio to the NO_y sum are shown in Figures 3a (nonplume) and 3b (within plumes). In the nonplume data the ratio NO_x/NO_y sum is 10-15% from the boundary layer to 7 km altitude, and then it increases to 25% at 12 km. Owing to slightly larger NO_x mixing ratios in the plume data, especially above 5 km, the ratio NO_x/NO_y sum is ~8-10% from the boundary layer to 7 km, and then it again increases to 25% at 12 km. The opposite trend is seen for the alkyl nitrates, decreasing from ~30-40% in the boundary layer to ~5% above 3 km altitude. In the nonplume data the ratio was higher at all altitudes by about 3-5%, presumably driven by a stronger marine source for these species compared with combustion plumes over the South Pacific.

The ratio HNO_3/NO_y sum in the nonplume air parcels has a value

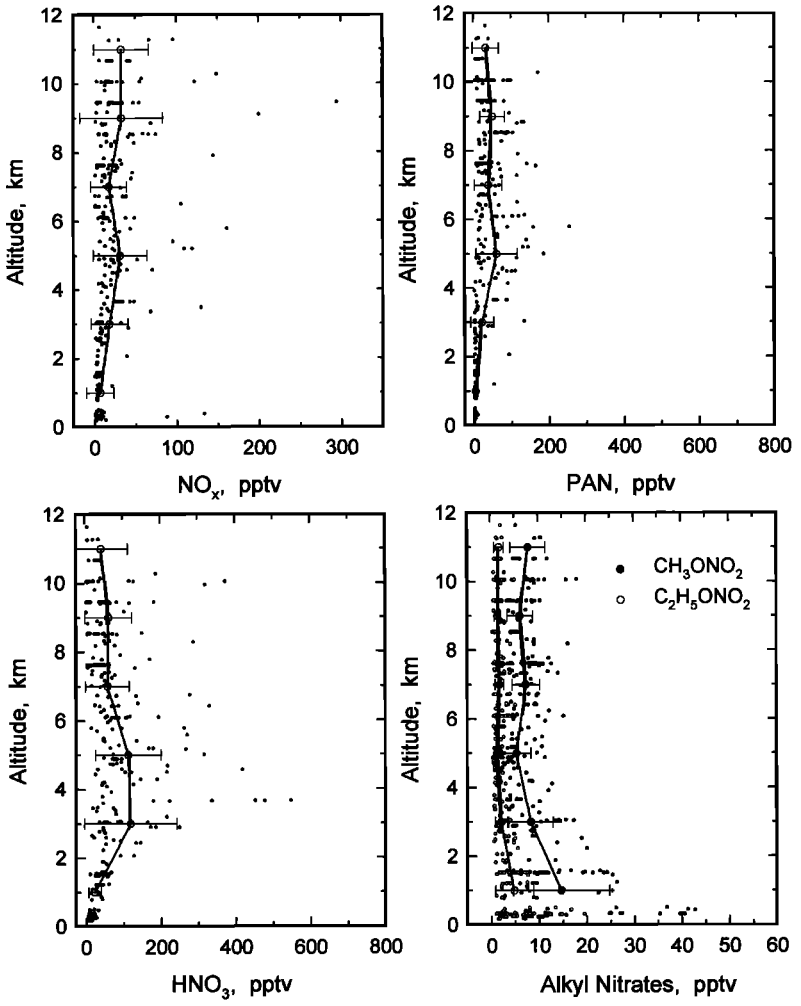

Figure 2a. Vertical distribution of reactive odd nitrogen species in nonplume air parcels over the South Pacific. The open circles represent the average value ± one standard deviation for 2 km altitude bins.

of ~50% in the boundary layer that increases to 70% in the 2-4 km region and then decreases linearly to ~25% at 12 km altitude. The sharp increase in the value of this ratio near 3 km may reflect the influence of cloud processes in this layer. Small cumulus with bases at the top of the marine boundary layer (1-1.5 km) may be releasing soluble gases to the gas phase as cloud tops in this transition layer dissipate at 3-4 km. Chemical and dynamical processes in this cloudy region are known to produce aerosols [*Clarke et al.*, 1999], and it seems likely that soluble gases would also be released by these same mechanisms. In the plume air parcels this effect is less noticeable due to elevated mixing ratios in and above this region. The ratio HNO_3/NO_y sum is still ~50% in the boundary layer, but this value is maintained up to 6 km before decreasing to ~40% at 12 km altitude. Thus there is a major impact on the NO_y partitioning above the marine boundary layer attributed to combustion/lightning inputs of reactive nitrogen.

The impact of the same inputs on the PAN/NO_y sum is less, even in the middle troposphere. This ratio is 5-10% in the boundary layer, increasing to 30-40% in the middle troposphere before decreasing to ~20% at 12 km altitude. In the middle troposphere, long-range transport appears to increase the ratio PAN/NO_y sum by about 10% in the plume air parcels compared with the nonplume cases.

4. Species Interrelationships

Comparisons between the nonplume and plume data sets shows that a very similar combustion influence is present in both air parcel classifications. Various species interrelationships demonstrate this point in Plate 2. In each of the correlations shown in Plate 2 the nonplume and plume distributions overlap fairly tightly, with the highest mixing ratios of C_2H_2, and the other parameters associated with the plume air parcels. The correlation of CH_3Cl and C_2H_2 indicates that a biomass burning source is responsible for at least some portion of the chemical signatures. The lack of similar correlation of C_2H_2 with industrial tracers (e.g., Figure 1) suggests that the combustion influence is mainly derived from biomass burning.

As can be seen in Plate 2, there was a substantial amount of O_3 associated with these plumes, a chemical characteristic of biomass burning emissions from South American and Africa [*Fishman and Brackett*, 1997]. In fact, about half of the O_3 in the tropospheric column over the South Pacific appears to have been advected eastward in biomass burning emissions from South America and Africa [*Schultz et al.*, 1999]. The apparent dispersion of these emissions throughout most of the tropospheric column over the South Pacific is likely due to mixing and dilution of combustion

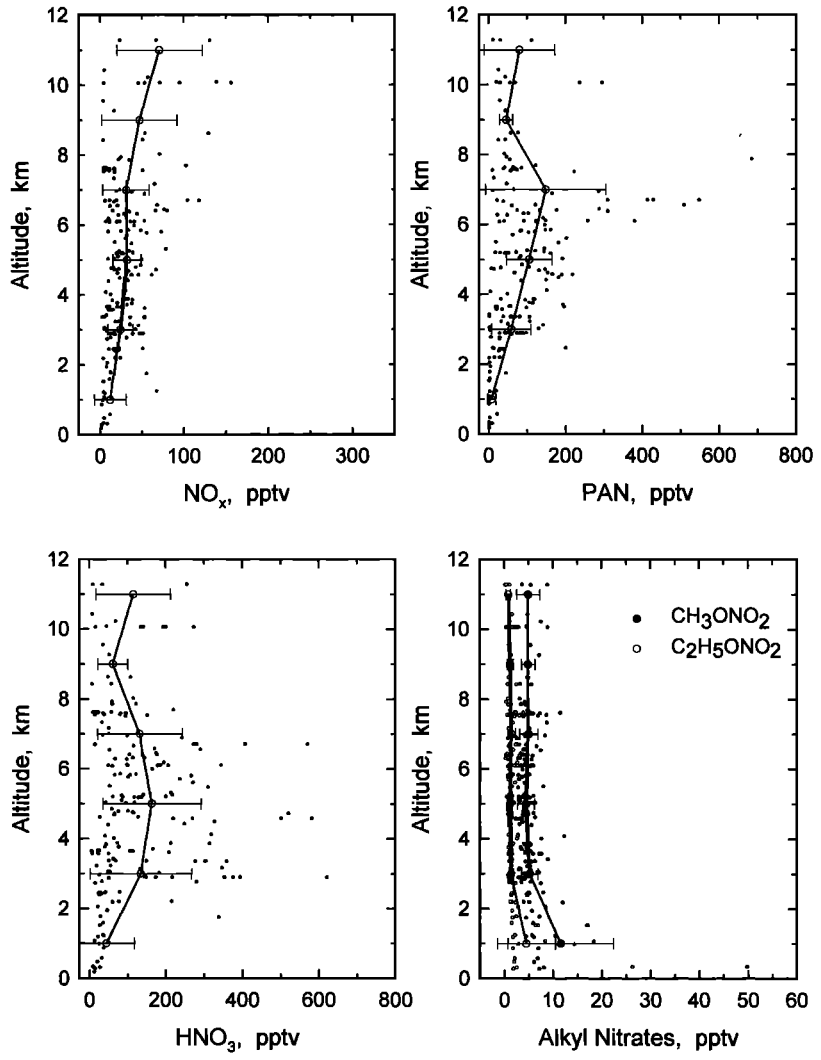

Figure 2b. Vertical distribution of reactive odd nitrogen species in combustion plumes over the South Pacific. The open circles represent the average value ± one standard deviation for 2 km altitude bins.

plumes with surrounding ambient air. The nonplume data chemical signature reflects this combustion influence. This is particularly pronounced for the NO_y sum, where data from both data classifications overlap significantly. The wide scatter in the C_2H_2/NO_y sum relationship is probably driven to a large degree by varying loss or production of HNO_3 and PAN. Plots of these two species against C_2H_2 (not shown) show scatter similar to that for the NO_y sum.

The relationships of CH_3Cl with PAN and the NO_y sum are presented in Plate 3. The extensive scatter in the relationship for the NO_y sum is similar to that with C_2H_2 (Plate 2). Slightly better correlation is found for PAN ($r^2 = 0.35$), but it is driven mainly by the highest values in both species. The GTE program investigated the chemical environment over the South Atlantic during the 1992 austral spring. Biomass burning pollution was evident throughout the tropospheric column, with CH_3Cl mixing ratios in the 600-700 pptv range [*Talbot et al.*, 1996b]. If we take a value of 650 pptv over the biomass burning source areas and 560 pptv over the South Pacific, this represents a 14% decrease in CH_3Cl over about a 2-week period. Attack by OH (at, say, 1×10^6 cm^{-3}) can account for maybe half of this drop, with the rest attributed to dilution. These rough estimates are consistent with other air mass history analyses, where OH attack and dilution were found to be equally responsible for decreases in hydrocarbon species [e.g., *McKeen and Liu*, 1993]. Thus the mixing ratios of CH_3Cl over the South Pacific are in the range expected for a South American/African biomass burning source.

These same air parcels could have had inputs of reactive nitrogen besides that from biomass burning. In some cases, lightning may have provided an additional source of reactive nitrogen. Additionally, we cannot rule out the stratosphere as a source of reactive nitrogen. Levels of ^7Be, a reasonably good stratospheric tracer in the troposphere, frequently exceeded 400 fCi (10^{-15} Ci) m^{-3} throughout much of the tropospheric column (Plate 4). Such concentrations of ^7Be are quite elevated, being 2-3 times higher than we have observed previously over the North Pacific [*Talbot et al.*, 1996a, 1997b]. Even though the correlation of the NO_y sum with ^7Be is not very robust (Plate 4), the high ^7Be concentrations still leave open the possibility that the stratosphere could have been a source of reactive nitrogen. A somewhat better correlation (a second-order fit gives $r^2 = 0.41$) is found between the NO_y sum and ^{210}Pb, a tracer of

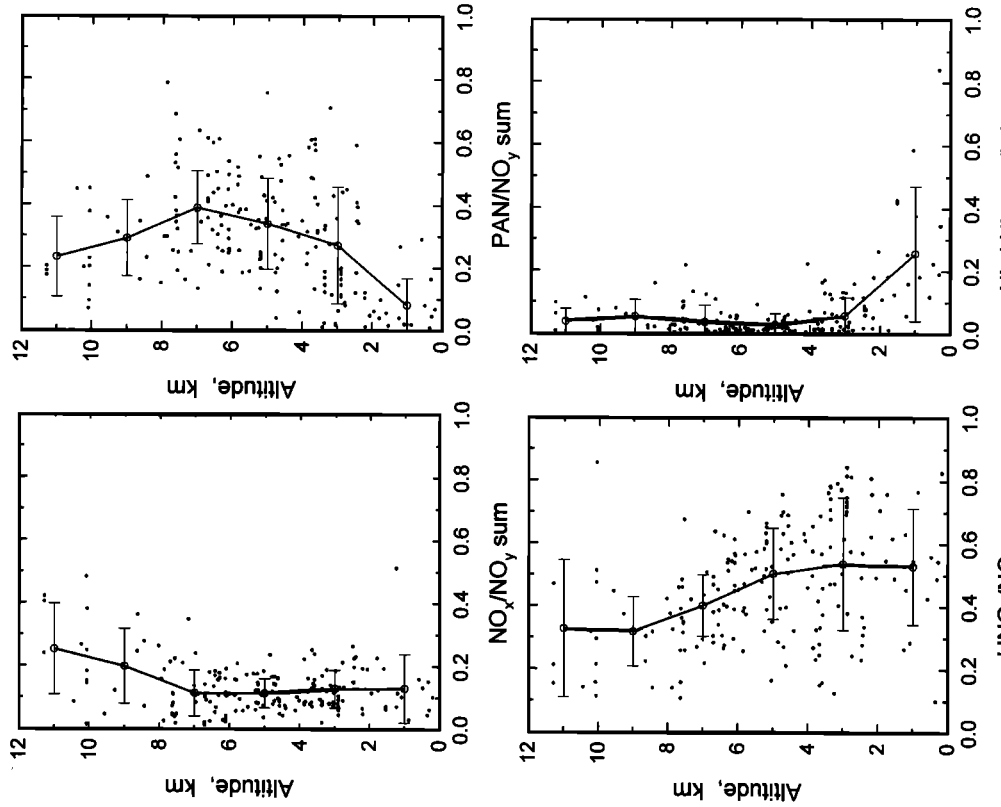

Figure 3b. Ratio of reactive odd nitrogen species to the NO_y sum in combustion plumes over the South Pacific. The open circles represent the average value ± one standard deviation for 2 km altitude bins.

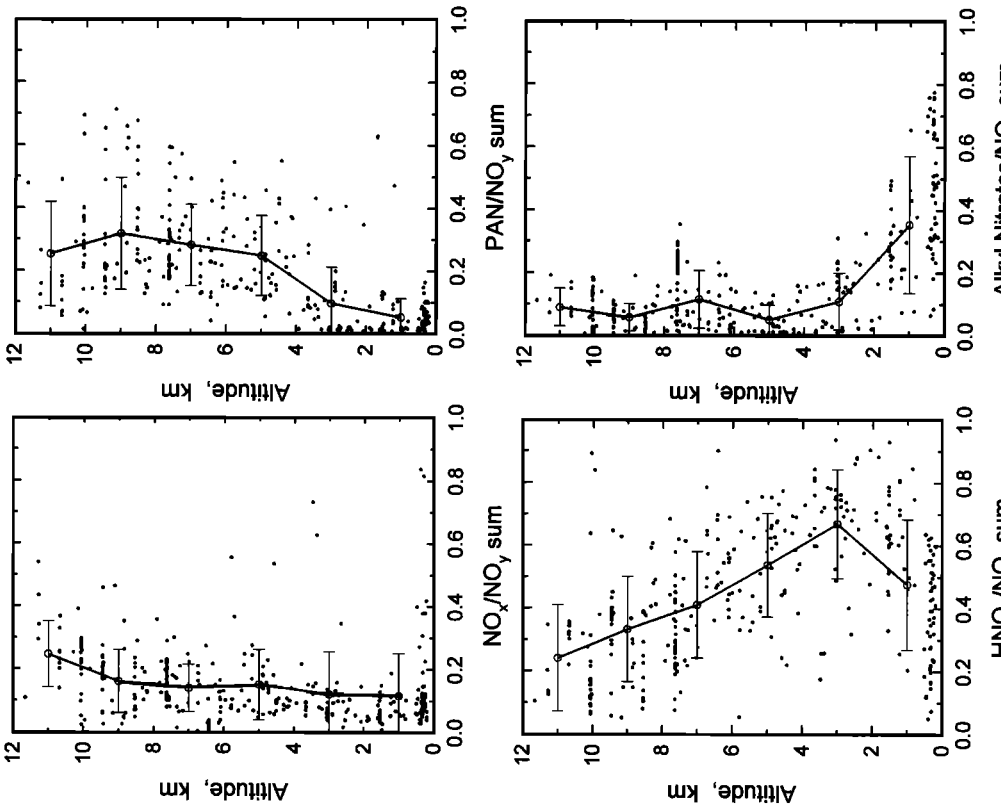

Figure 3a. Ratio of reactive odd nitrogen species to the NO_y sum in nonplume air parcels over the South Pacific. The open circles represent the average value ± one standard deviation for 2 km altitude bins.

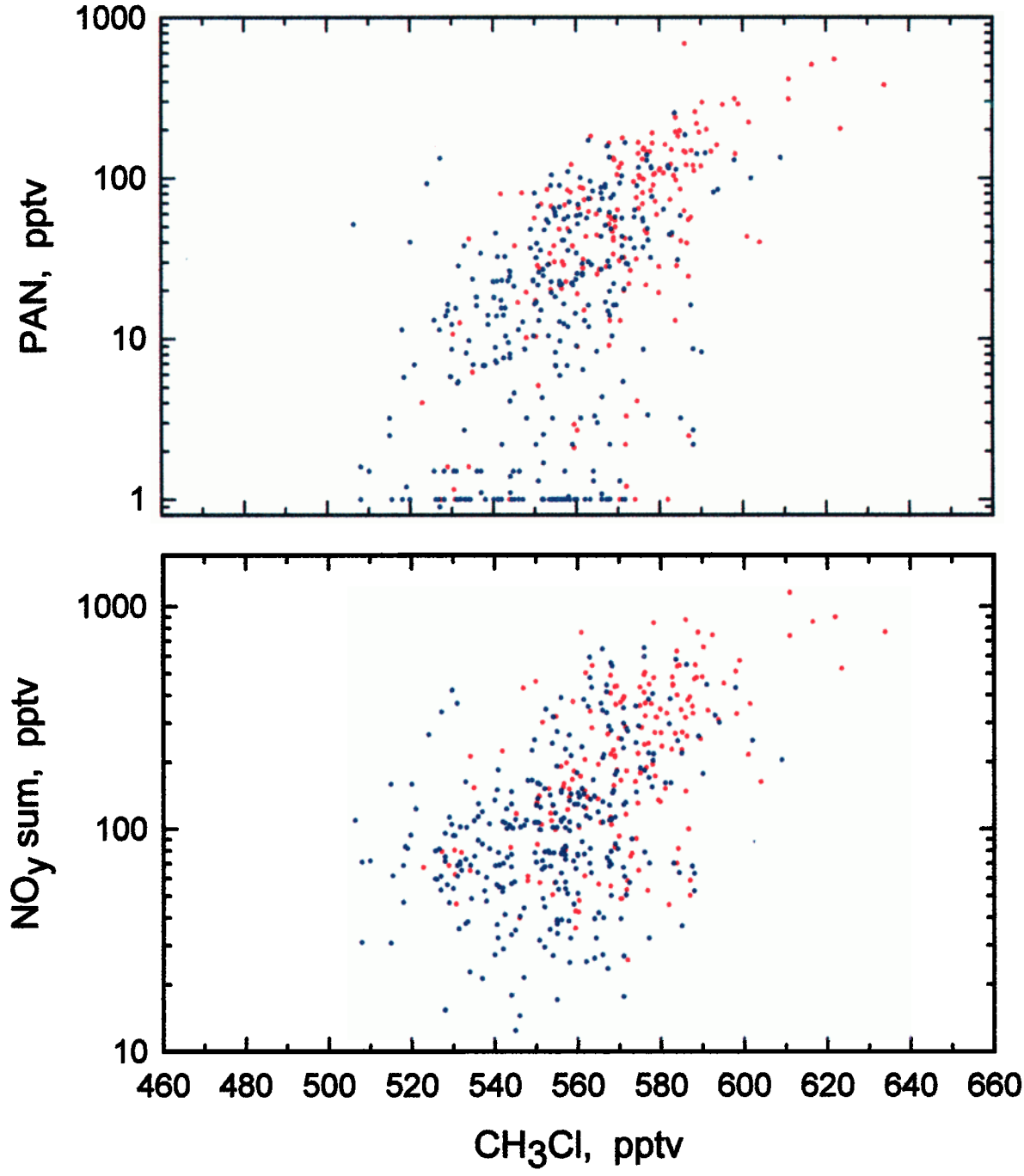

Plate 3. Relationship between PAN and the NO_y sum with CH_3Cl over the South Pacific. Blue dots are nonplume data, and red dots are from within combustion plumes. Note that the plot has a semilogarithmic scale.

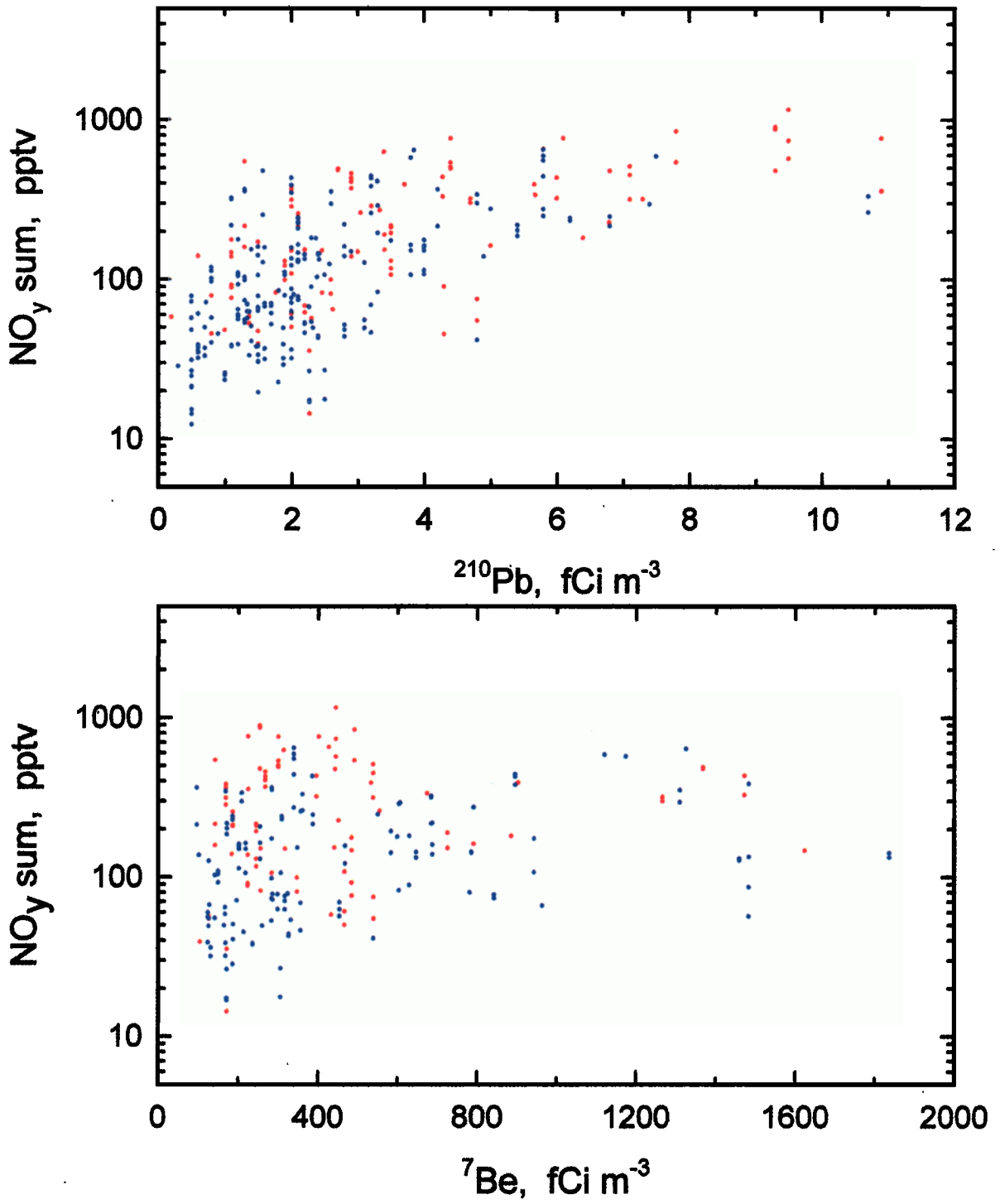

Plate 4. Relationship between the NO_y sum and ^{210}Pb, a continental tracer, and ^{7}Be, a tracer of stratospheric inputs to the troposphere. Blue dots are nonplume data, and red dots are from within combustion plumes. Note that the plot has a semilogarithmic scale.

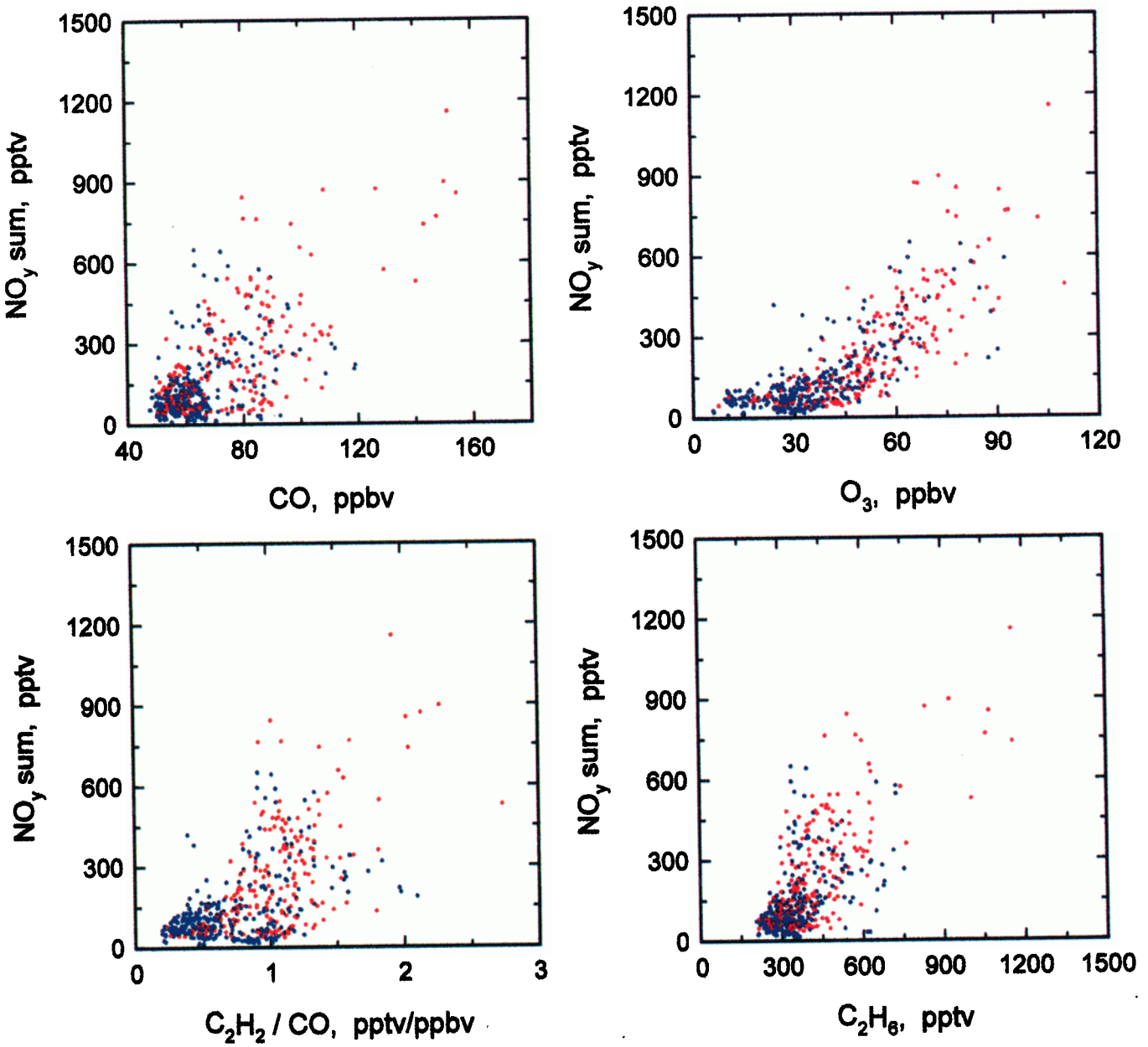

Plate 5. Relationship of the NO_y sum to selected pollution-associated species over the South Pacific. Blue dots are nonplume data, and red dots are from within combustion plumes.

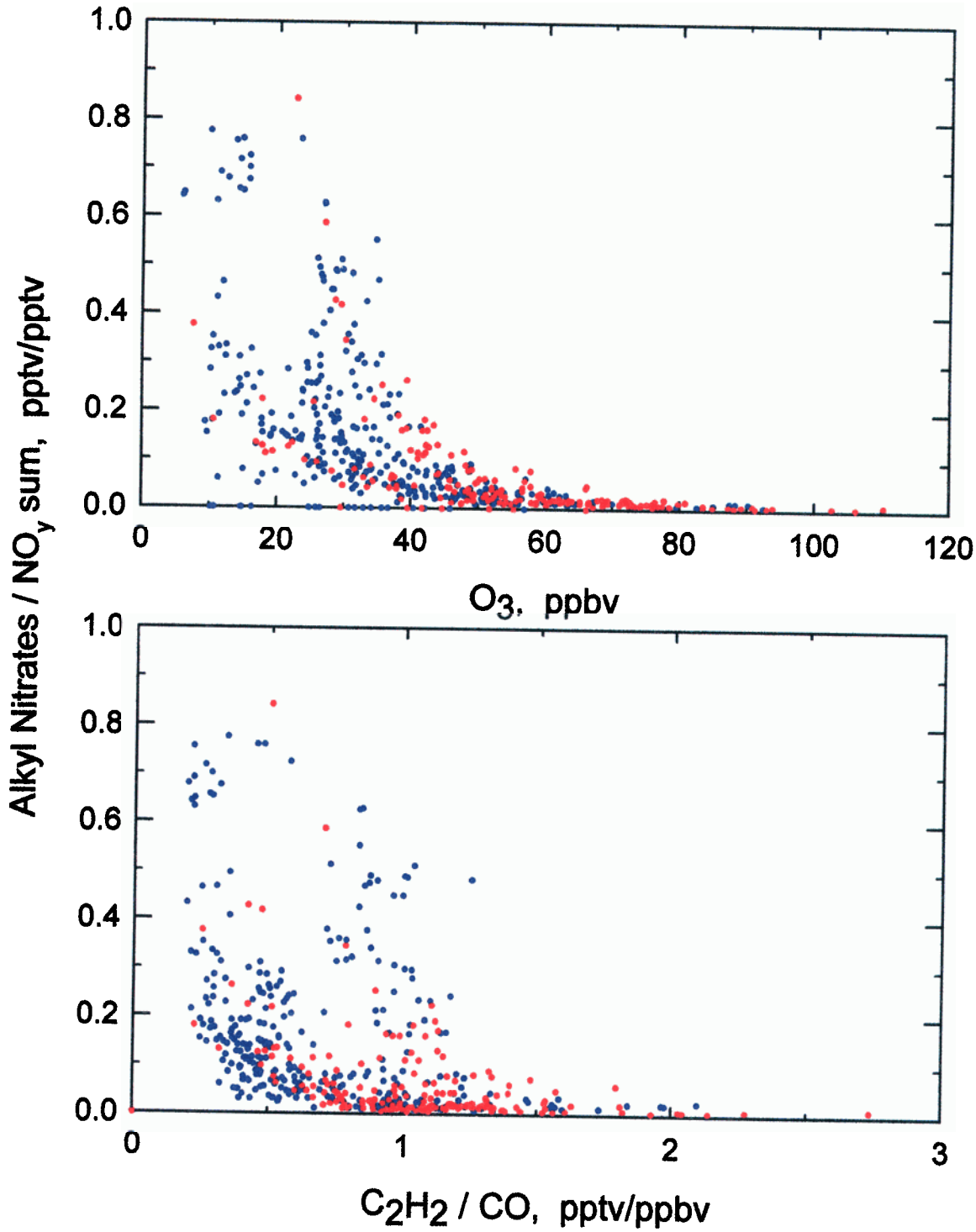

Plate 6. Ratio of alkyl nitrates ($CH_3ONO_2 + C_2H_5ONO_2$) to the NO_y sum as a function of O_3 and C_2H_2/CO. Blue dots are nonplume data, and red dots are from within combustion plumes.

continental emissions [*Dibb et al.*, 1996]. Both data classifications support this relationship, endorsing the idea that the chemistry of the nonplume air parcels was strongly influenced by plume dissipation. This correlation indicates that continental combustion emissions were probably an important source of the NO_y sum, but the distinction between combustion and lightning inputs cannot be uniquely resolved. With possible multiple sources of the NO_y sum without concomitant CH_3Cl inputs, its not surprising that the correlation in these two species is weak over the South Pacific (Plate 3).

Relationships of the NO_y sum with other selected parameters are depicted in Plate 5. As with CH_3Cl, the relationships exhibit significant scatter except for that with O_3. Again, we attribute this scatter to multiple possible sources for the NO_y sum and the aged nature of the air parcels from dilution and OH decomposition of CO and hydrocarbons. Despite the fact that well-defined relationships are not present, it is clear that the most aged air parcels with C_2H_2/CO ratios <0.5 contain the lowest mixing ratios of the NO_y sum. The majority of the nonplume data fall into this category, where most of the reactive nitrogen has probably been converted to HNO_3 and subsequently lost from the atmosphere by wet and dry deposition processes.

Quite a different picture appears to be plausible for the alkyl nitrate species. In this case they appear to comprise the largest fraction of the NO_y sum coincident with the smallest mixing ratios of O_3 and values of the ratio C_2H_2/CO (Plate 6). This, of course, corresponds to air parcels in the marine boundary layer which contain direct marine emissions of alkyl nitrates and are somewhat isolated from the air above (by temperature inversions), are photochemically aged (low C_2H_2/CO), and contain low O_3 due to chemical and surface deposition losses. It should be noted that aerosol NO_3^- mixing ratios were very similar to those for the alkyl nitrates in the marine boundary layer, generally ranging from 20 to 50 pptv [*Dibb et al.*, 1999a]. Thus these nitrate compounds together comprise nearly all of the NO_y sum in this lower tropospheric region.

In the most aged air masses sampled with C_2H_2/CO<0.5, alkyl nitrates often composed >20% of the NO_y sum. The majority of the alkyl nitrate plume data contained low mixing ratios and ratio values to the NO_y sum. The majority of the data with the greatest alkyl nitrate/NO_y sum ratios were in the nonplume air parcel classification. There appear to be two different distributions, one with C_2H_2/CO ratio values <0.5 and the other with a ratio value of ~1.0 (Plate 6). Most of the data associated with ratio values around 1.0 were collected at high latitude (50°-70°S) during a flight south of New Zealand to Antarctica where the NO_y sum was <70 pptv. The other distributions at lower C_2H_2/CO ratio values are from flights in the tropical South Pacific region. Thus it appears that alkyl nitrates are important reactive nitrogen species in the marine boundary layer in equatorial and high-latitude regions of the Pacific Ocean. Although this point has been speculated on previously [*Atlas*, 1988], the PEM-Tropics A data are a first definitive demonstration of it.

5. Conclusion

This paper presents the distribution of reactive odd nitrogen species over the South Pacific Ocean during austral springtime. Mixing ratios of NO_x were generally low (<20 pptv) throughout the tropospheric column (0-12.5 km), with little evidence for a dominant source. The absence of clear chemical signatures correlated with the NO_x distribution is attributed to the 1- to 2.5-week-old age of the sampled air parcels. The distributions of HNO_3 and PAN indicate an important biomass burning source for reactive nitrogen in the free troposphere, although contributions from lightning and the stratosphere cannot be ruled out. In the marine boundary layer, alkyl nitrate species are a major component of the NO_y sum, with this natural oceanic source especially important in equatorial and high-latitude regions.

Acknowledgments This research was sponsored by the NASA Tropospheric Chemistry Program We appreciate the excellent support provided by the NASA Ames DC-8 flight and ground crews.

References

Atlas, E., Evidence for ≥C3 alkyl nitrates in rural and remote atmospheres, *Nature, 331*, 426-428, 1988.

Atlas, E. L., B. A. Ridley, G. Hübler, J. G. Walega, M. A. Carroll, D. D. Montzka, B. J. Huebert, R. B. Norton, F E. Grahek, and S. Schauffler, Partitioning and budget of NO_y species during the Mauna Loa Observatory Photochemistry Experiment, *J. Geophys. Res., 97*, 10,449-10,462, 1992a.

Atlas, E., S. M Schauffler, J. T. Merrill, C. J. Hahn, B. Ridley, J. Walega, J. Greenberg, L. Heidt, and P. Zimmerman, Alkyl nitrate and selected halocarbon measurements at Mauna Loa Observatory, Hawaii, *J. Geophys. Res., 97*, 10,331-10,348, 1992b.

Blake, D. R., T.-Y. Chen, T. W. Smith Jr., C. J.-L. Wang, O. W. Wingenter, N. J. Blake, and F. S. Rowland, Three-dimensional distribution of nonmethane hydrocarbons and halocarbons over the northwestern Pacific during the 1991 Pacific Exploratory Mission (PEM-West A), *J. Geophys Res., 101*, 1763-1778, 1996a.

Blake, N. J., D. R. Blake, B. C. Sive, T.-Y. Chen, F. S. Rowland, J.E. Collins Jr., G.W. Sachse, and B.E. Anderson, Biomass burning emissions and vertical distribution of atmospheric methyl halides and other reduced carbon gases in the South Atlantic region, *J. Geophys. Res., 101*, 24,151-24,164, 1996b

Blake, N. J , et al., Influence of southern hemispheric biomass burning on midtropospheric distributions of nonmethane hydrocarbons and selected halocarbons over the remote South Pacific, *J. Geophys. Res., 104*, 16,213-16,232, 1999.

Bradshaw, J. D., M. O. Rogers, S. T Sandholm, S. KeSheng, and D D. Davis, A two-photon laser-induced fluorescence field instrument for ground-based and airborne measurements of atmospheric NO, *J. Geophys. Res., 90*, 12,861-12,873, 1985.

Bradshaw, J D., S. T. Sandholm, and R W. Talbot, An update on reactive odd nitrogen measurements made during recent NASA Global Tropospheric Experiment programs, *J Geophys. Res., 103*, 19,129-19,148, 1998.

Bradshaw, J. D., et al., Photofragmentation two-photon laser-induced fluorescence detection of NO_2 and NO Comparison of measurements with model results based on airborne observations during PEM-Tropics A, *Geophys. Res. Lett , 26*, 471-474, 1999.

Clarke, A. D., F. Eisele, V. N. Kapustin, K. Moore, D. Tanner, L. Mauldin, M. Litchy, B. Lienert, M. A. Carroll, and G. Albercook, Nucleation in the free troposphere. Favorable environments during PEM-Tropics, *J. Geophys. Res., 104*, 5735-5744, 1999.

Dibb, J. E., R. W. Talbot, K. I. Klemm, G. L Gregory, H. B Singh, J. D. Bradshaw, and S. T. Sandholm, Asian influence over the western North Pacific during the fall season: Inferences from lead 210, soluble ionic species and ozone, *J. Geophys. Res., 101*, 1779-1792, 1996.

Dibb, J. E., R. W Talbot, E. M. Scheuer, D. R. Blake, N. J Blake, G. L. Gregory, G W. Sachse, and D. C. Thornton, Aerosol chemical composition and distribution during the Pacific Exploratory Mission (PEM) Tropics, *J. Geophys. Res., 104*, 5785-5800, 1999a.

Dibb, J. E., R. W. Talbot, L. D. Meeker, E. M. Scheuer, N. J. Blake, D. R. Blake, G. L. Gregory, and G. W Sachse, Constraints on the age and dilution of Pacific Exploratory Mission-Tropics biomass burning plumes from the natural radionuclide tracer ^{210}Pb, *J. Geophys. Res., 104*, 16,233-16,241, 1999b.

Fahey, D. W., G. Hübler, D. D. Parrish, E. J. Williams, R B. Norton, B. A. Ridley, H. B. Singh, S. C. Liu, and F. C. Fehsenfeld, Reactive nitrogen species in the troposphere Measurements of NO, NO_2, HNO_3, particulate nitrate, peroxyacetyl nitrate (PAN), O_3, and total reactive odd nitrogen (NO_y) at Niwot Ridge, Colorado, *J. Geophys. Res., 91*, 9781-9793, 1986.

Fishman, J., and V. G. Brackett, The climatological distribution of tropospheric ozone derived from satellite measurements using version 7 Total Ozone Mapping Spectrometer and Stratospheric Aerosol and Gas Experiment data sets, *J. Geophys. Res.*, *102*, 19,275-19,278, 1997.

Fuelberg, H. E., R. E. Newell, S. Longmore, Y. Zhu, D. J. Westberg, E.V. Browell, D.R. Blake, G.L. Gregory, and G.W. Sachse, A meteorological overview of the Pacific Exploratory Mission (PEM) Tropics period, *J. Geophys. Res.*, *104*, 5585-5622, 1999.

Gregory, G. L., J. M. Hoell Jr., B. A Ridley, H. B Singh, B. Gandrud, L. J. Salas, and J. Shetter, An intercomparison of airborne PAN measurements, *J. Geophys. Res.*, *95*, 10,077-10,087, 1990.

Gregory, G. L., et al., Chemical characteristics of Pacific tropospheric air in the region of the Intertropical Convergence Zone and South Pacific Convergence Zone, *J. Geophys. Res.*, *104*, 5677-5696, 1999.

Hoell, J. M., D. D. Davis, D. J. Jacob, M. O. Rodgers, R. E. Newell, H. E. Fuelberg, R. J. McNeal, J. L. Raper, and R. J. Bendura, Pacific Exploratory Mission in the tropical Pacific: PEM-Tropics A, August-September 1996, *J. Geophys. Res.*, *104*, 5567-5583, 1999.

Kasting, J. F., and H. B. Singh, Nonmethane hydrocarbons in the trospophere: Impact on odd hydrogen and odd nitrogen chemistry, *J. Geophys. Res.*, *91*, 13,239-13,256, 1986.

Kliner, D. A. V., B. C. Daube, J. D. Burley, and S. C. Wofsy, Laboratory investigation of the catalytic reduction technique for measurement of atmospheric NO_y, *J. Geophys. Res.*, *102*, 10,759-10,776, 1997.

Logan, J. A., Nitrogen oxides in the troposphere: Global and regional budgets, *J. Geophys. Res.*, *88*, 10,785-10,807, 1983.

McKeen, S. A., and S. C. Liu, Hydrocarbon ratios and photochemical history of air masses, *Geophys. Res. Lett.*, *20*, 2363-2366, 1993.

Ridley, B. A., Recent measurements of oxidized nitrogen compounds in the troposphere, *Atmos. Environ.*, *25*, 1905-1926, 1991.

Sandholm, S. T., J. D. Bradshaw, K. S. Dorris, M. O. Rogers, and D. D. Davis, An airborne compatible photofragmentation two-photon laser-induced fluorescence instrument for measuring background tropospheric levels of NO, NO_x, and NO_2, *J. Geophys. Res* , *95*, 10,155-10,161, 1990.

Sandholm, S. T., et al., Summertime partitioning and budget of NO_y compounds in the troposphere over Alaska and Canada: ABLE 3B, *J. Geophys. Res* , *99*, 1837-1861, 1994.

Schultz, M. G., et al., On the origin of tropospheric ozone and NO_x over the tropical South Pacific, *J. Geophys. Res.*, *104*, 5829-5843, 1999.

Singh, H. B., and L. J. Salas, Methodology for the analyses of peroxyacetyl nitrate (PAN) in the unpolluted atmosphere, *Atmos. Environ.*, *17*, 1507-1516, 1983.

Talbot, R. W., et al., Chemical characteristics of continental outflow from Asia to the troposphere over the western Pacific Ocean during September-October 1991: Results from PEM-West A, *J. Geophys. Res.*, *101*, 1713-1725, 1996a.

Talbot, R. W., et al., Chemical characteristics of continental outflow over the tropical South Atlantic Ocean from Brazil and Africa, *J. Geophys. Res.*, *101*, 24,187-24,202, 1996b

Talbot, R. W , et al., Large-scale distributions of tropospheric nitric, formic, and acetic acids over the western Pacific basin during wintertime, *J. Geophys. Res.*, *102*, 28,303-28,313, 1997a.

Talbot, R. W., et al., Chemical characteristics of continental outflow from Asia to the troposphere over the western Pacific Ocean during February-March 1994: Results from PEM-West B, *J. Geophys. Res.*, *102*, 28,255-28,274, 1997b.

Talbot, R. W., et al., Reactive nitrogen budget during the NASA SONEX mission, *Geophys. Res. Lett.*, 26, 3057-3060, 1999a.

Talbot, R. W., J. E. Dibb, E. M. Scheuer, D. R. Blake, N. J. Blake, G. L. Gregory, G. W. Sachse, J. D. Bradshaw, S. T. Sandholm, and H. B Singh, Influence of biomass combustion emissions on the distribution of acidic trace gases over the southern Pacific basin during austral springtime, *J. Geophys. Res.*, *104*, 5623-5634, 1999b.

E. Atlas and F. Flocke, Atmospheric Chemistry Division, National Center for Atmospheric Research, Boulder, CO 80303. (Atlas@ucar.edu; ffl@ucar.edu)

D. R. Blake and N. J. Blake, Department of Chemistry, University of California, Irvine, Irvine, CA 92697. (dblake@orion oac.uci.edu; nblake@orion.oac.uci.edu)

J. E Dibb, E. M. Scheuer, and R. W. Talbot, Institute for the Study of Earth, Oceans, and Space, University of New Hampshire, Durham, NH 03824. (jack.dibb@unh.edu; eric.scheuer@unh.edu; robert.talbot@unh.edu)

S. T. Sandholm, Department of Earth and Atmospheric Sciences, Georgia Institute of Technology, Atlanta, GA 30322. (scott.sandholm@eas.gatech.edu)

H. B. Singh, NASA Ames Resesarch Center, Moffett Field, CA 94035. (hsingh@mail.arc.nasa.gov)

(Received August 3, 1999; revised November 1, 1999;
accepted November 4, 1999.)